

Classifying Subjective Time Perception in a Multi-robot Control Scenario Using Eye-tracking Information

Till Aust,¹ Julian Kaduk,¹ and Heiko Hamann^{1,2}

Abstract—As automation and mobile robotics reshape work environments, rising expectations for productivity increase cognitive demands on human operators, leading to potential stress and cognitive overload. Accurately assessing an operator’s mental state is critical for maintaining performance and well-being. We use subjective time perception, which can be altered by stress and cognitive load, as a sensitive, low-latency indicator of well-being and cognitive strain. Distortions in time perception can affect decision-making, reaction times, and overall task effectiveness, making it a valuable metric for adaptive human-swarm interaction systems.

We study how human physiological signals can be used to estimate a person’s subjective time perception in a human-swarm interaction scenario as example. A human operator needs to guide and control a swarm of small mobile robots. We obtain eye-tracking data that is classified for subjective time perception based on questionnaire data. Our results show that we successfully estimate a person’s time perception from eye-tracking data. The approach can profit from individual-based pretraining using only 30 seconds of data. In future work, we aim for robots that respond to human operator needs by automatically classifying physiological data in a closed control loop.

I. INTRODUCTION

In today’s rapidly evolving work environments, driven increasingly by automation, prioritizing the mental health of the workforce is becoming essential [1]. Workplace stressors can negatively impact well-being, decrease productivity, and potentially lead to burnout. A potential indicator is subjective time perception, which may be experienced as slower under stress [2]. When a person is positively engaged, they tend to perceive time as passing more quickly.

In our project *ChronoPilot* [3], we attempt to actively modulate time perception of workers in virtual (VR) or augmented reality (AR) automation scenarios in order to increase their well-being and productivity. We aim to develop a device that both adjusts time perception and simultaneously measures the user state by obtaining human feedback. We modulate users’ time perception through haptic [4], visual [5] auditory [6], or situational stimuli [7]. A user’s time perception state can be estimated by non-invasively measuring their physiological signals [8], [9]. A promising physiological signal is eye-tracking due to its great availability, minimal intrusiveness, and reliable measurement across a variety of settings [10]. Many current and future tasks/jobs can be performed or supported using VR or AR devices, such as the

Vision Pro¹ or Meta Quest 3.² These devices capture eye-tracking data as part of their functionality, hence, requiring no additional hardware. One such task, considering the rise of mobile robots, multi-robot systems, and swarm robotics [11], [12], could be to guide or control semi-autonomous groups of robots. This human-robot interaction or even more so human-swarm interaction [13], [14] may have high demands for a human operator and may potentially be stressful. Research has shown that passively observing [15] or controlling [16] a larger number of robots moving around, and also smoothness in robot motion [17] can influence the participant’s well-being. Participants reported a faster passage of time when controlling a larger number of robots [7].

Possible approaches to moderating stressful effects of controlling a robot swarm include the use of automated after-action reviews [18] or monitoring the participants’ heart rate variability (HRV) [19]. In automated after-action reviews, the human-robot task is replayed to the participant directly after execution and questionnaires need to be filled. This is not applicable in our case, as we aim to monitor the time perception online in order to actively modify the work environment. Moreover, interrupting the task to review time perception may skew the results as by disturbing the participant’s workflow. Instead, measurements should occur in parallel with the participant’s task, ideally without the participant’s conscious awareness. We prefer to use the participant’s physiological data, such as HRV and eye-tracking. A common approach to process eye-tracking data is to extract features, such as the pupil size, eye movement, or blinking. These are compiled into a feature vector and classified using machine learning (ML) algorithms [20]. Utilizing this approach, eye-tracking information can be used to detect stress [21], monitor mental workload [22], or recognize emotion [23].

A common limitation of these studies is the ad hoc selection of ML models, with no clear rationale for choosing one over another. Model selection often seems to rely on manual parameter tuning or comparisons within a limited set of models, lacking a systematic approach. Using automated machine learning (AutoML) is a potential solution providing justification and ensuring thorough exploration of search spaces for ML models and their hyperparameter configurations. AutoML methods automatically compose ML algorithms into a pipeline and choose appropriate hyperparameters to optimize a given metric [24]. Existing frameworks like *auto-sklearn* [25], [26] and GAMA [27] provide ready-

¹Till Aust, Julian Kaduk and Heiko Hamann are with the Department of Computer and Information Science, University of Konstanz, Konstanz, Germany. till.aust@uni-konstanz.de

²Heiko Hamann is member of the Centre for the Advanced Study of Collective Behaviour (CASCB), Universität Konstanz, Konstanz, Germany

¹<https://www.apple.com/de/apple-vision-pro/>

²<https://www.meta.com/de/quest/quest-3/>



Fig. 1: POV of participant during the robot experiment.

to-use implementations. More recently, *Mohr and Wever* [28] introduced the Naive AutoML framework, which achieves comparable performance with a substantial reduction in computation time. In this paper, we study how to derive subjective time perception feedback from eye-tracking data obtained during a multi-robot controlling scenario, using an automated ML approach based on Naive AutoML [28], with the goal of closing the feedback loop of the *ChronoPilot* device.

II. EXPERIMENTS AND METHODOLOGY

The eye-tracking data were collected in robot experiments with participants controlling a robot swarm [16]. We preprocess the eye-tracking data for an AutoML approach to optimize an ML pipeline and its hyperparameters.

A. Robot experiment

Participants control a swarm of small mobile robots (Thymio II [29]) using a single-button interface (see Fig. 1) across 24 randomized trials, while eye-tracking and questionnaires capture physiological responses and perceived time during varying trial durations and counts of active robots. A more detailed description is given by Kaduk *et al.* [16].

In the experiment, we differentiate between active and passive robots. The active robots follow a random walk with obstacle avoidance and user input, while the passive robots are stationary at random locations. The participant has a single-button interface with the task to keep all active robots within a rectangle (2.2 m by 1.6 m) marked by black tape on the floor. When the button is pressed, all active robots rotate on the spot in random direction until either the button is released or a 3-second timer has elapsed. The experiment was split into 24 different trials randomized in order for each participant. The two variable parameters were the trial duration of either 1 min, 3 min, or 5 min and the number of actively moving robots $N_{\text{active}} \in \{1, 3, \dots, 15\}$. Before each trial, the participant was asked to watch a relaxing aquatic video for two minutes to provide a neutral baseline of the physiological data [30]. Each participant completed these trials during two appointments of approximately 1.5 hours each. The participants were equipped with a Pupil Core eye-tracking platform.³ After each trial, the participant filled in a questionnaire including estimates of their subjective

perceived passage of time (PPOT) on a 5-point Likert scale and the duration of the experiment on a visual timeline ranging from 0:00 to 10:00 minutes.

B. Eye-tracking data

All experiment data were recorded with synchronized timestamps using the lab steaming layer [31] and the Pupil Labs software (also used for calibration of the Pupil Core eye-tracking device). The timestamps were used to split the data into individual trial sequences. A total of 21 participants completed the 24 trials each, yielding 504 experiment sequences. Due to software malfunctions and calibration losses, 99 sequences (19.6%) were excluded from analysis.

All sequences contain the normalized x and y position of the pupil center, the 2-dimensional pupil diameter for the left and right eye, the 3-dimensional pupil diameter for the left and right eye, the fixation ID (indicating the number of fixations), the normalized x and y position of the fixation, the dispersion, and the duration recorded by the Pupil Core eye-tracking platform.

The remaining 405 experiment eye-tracking sequences are divided into non-overlapping slices of $t_w = \{1 \text{ s}, 2 \text{ s}, 5 \text{ s}, 10 \text{ s}, 15 \text{ s}, 20 \text{ s}, 30 \text{ s}, 45 \text{ s}, 60 \text{ s}\}$ (extending the time window selection of [22]). Subsequently, the sliced sequences and the baseline sequences are used to calculate the features.

From the sequences, we extract 26 features that are grouped into features related to eye movement (total of 10 features) and features related to pupillary response (total of 16 features). The features related to eye movement are: fixation frequency, fixation duration mean, fixation duration maximum, fixation dispersion mean, fixation dispersion maximum, saccade frequency, saccade duration mean, saccade duration maximum, saccade speed mean, and saccade speed maximum. The features related to pupillary response are: pupil diameter 2d mean/maximum/standard deviation for the left and right eye, pupil diameter 3d mean/maximum/standard deviation for the left and right eye, and index of pupillary activity (IPA) [32] derived from 2d and 3d for the left and right eye.

We apply baseline subtraction to all features calculated from the experiment sequences. We subtract the feature value derived from the baseline condition from the corresponding feature in the experiment data slice. This adjustment compensates for potential variation in illumination due to daytime or lamp settings, which can significantly impact the eye-tracking features [10] differently for each participant.

Finally, we split the dataset into an analysis dataset, which is used for training and cross-validation, and a test dataset which is used for the final performance evaluation. To ensure reproducibility, we have made the code publicly available.^{4,5}

C. Time perception labels

The participants' answers to the questionnaires after each experiment provide information to label the dataset. We have two labels "duration estimation," derived from the subjective

³<https://pupil-labs.com/products/core>

⁴https://github.com/tilly111/chronopilot_feature_extraction

⁵https://github.com/tilly111/chronopilot_classification

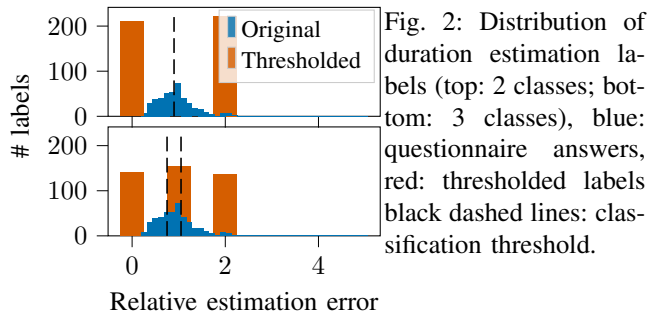


Fig. 2: Distribution of duration estimation labels (top: 2 classes; bottom: 3 classes), blue: questionnaire answers, red: thresholded labels, black dashed lines: classification threshold.

estimation of time, and subjective perceived passage of time (PPOT) which is estimated based on the questionnaire.

We either split the labels into a binary classification problem [8] or a three-class problem [9]. The binary classification is an essential benchmark that provides minimal feedback in potential applications. The three-class classification problem is interesting for our application of the *ChronoPilot* device. It provides all information (e.g., speed up, slow down, or keep as is) to decide whether and which stimulus needs to be applied to change the time perception of the user.

1) *Duration estimate*: After each experiment, participants estimated the duration of the experimental interaction on a visual timeline ranging from 0:00 to 10:00 minutes. The estimated duration was then divided by the actual experiment length (e.g., 1, 3, or 5 min) to compute the relative estimation error e_{rel} . For binary classification, we thresholded the relative estimation error e_{rel} at 0.9 categorizing values $e_{rel} \leq 0.9$ as underestimation and $e_{rel} > 0.9$ as overestimation. This threshold accounts for the general tendency toward underestimation as described by Vierodt’s law [33]. For three-class classification, we used thresholds of 0.75 and 1.05: $e_{rel} < 0.75$ is underestimation, $0.75 \leq e_{rel} \leq 1.05$ is interpreted as correct estimation, and $e_{rel} > 1.05$ is overestimation. Again, these thresholds address the general trend of underestimation. The distribution of labels is shown in Fig. 2.

2) *Subjective perceived passage of time*: The participants had to estimate their subjective passage of time after each experiment on a 5-point Likert scale ranging from “very slow” to “very fast.” For the binary classification task we thresholded “very slow” and “slow” to class slow subjective PPOT and “neutral,” “fast,” and “very fast” to class fast subjective PPOT (similar to [8]). For the three class classification problem we combined “very slow” and “slow” to class slow subjective PPOT, “neutral” to class neutral subjective PPOT, and “fast” and “very fast” to class fast subjective PPOT. An overview of the label distribution is shown in Fig. 3.

D. Automated machine learning

We utilize the Naive AutoML library [28] to automatically optimize ML pipelines for our eye-tracking data in a binary or three-class classification task using all eye-tracking features. Naive AutoML searches through *sci-kit learn* [34] classifier and preprocessing implementations to identify the classification pipeline that optimizes a given metric. This optimization follows a greedy approach in two phases: (1) identifying the best combination of pre-processors and

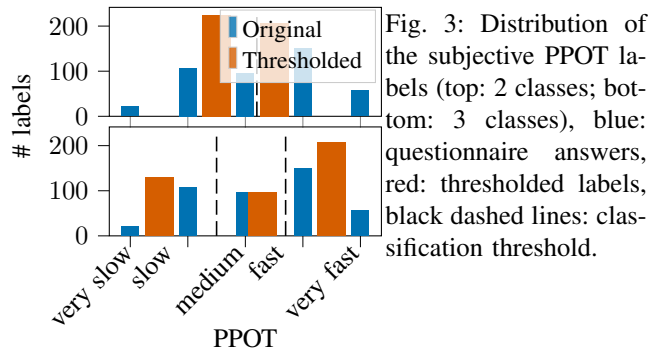


Fig. 3: Distribution of the subjective PPOT labels (top: 2 classes; bottom: 3 classes), blue: questionnaire answers, red: thresholded labels, black dashed lines: classification threshold.

classifiers with default hyperparameters via enumeration, discarding invalid combinations, and (2) optimizing the hyperparameters of the selected algorithms using random search (e.g., randomly selecting hyperparameters until a valid configuration is found in the default hyperparameter search space of Naive AutoML). After completing a predefined number of optimization steps, the best pipeline found is trained on the full dataset and returned. Although the greedy approach could potentially result in sub-optimal pipelines, empirical evidence shows that the performance of these solutions typically has little to no gap compared to those obtained by more time-consuming methods [28]. This library is highly configurable, enabling the setting of timeout limits, maximum hyperparameter iterations, and evaluation metrics. We do not set a timeout limit but restrict the optimization to 1024 hyperparameter steps and apply early stopping if there is no improvement after 100 iterations. Further, we excluded the histogram-based gradient boosting classifier as it did not work properly during the hyperparameter iterations. For evaluation we choose accuracy (ACC), because it will ultimately be the essential measure for our envisioned application and is applicable to both binary classification and three-class classification. In all cases, we took the default configuration of 5 independent and stratified 80%/20% training/validation splits of Naive AutoML to evaluate the ML pipelines.

III. RESULTS AND DISCUSSION

To use eye-tracking data for subjective time perception classification (e.g., feedback control of the *ChronoPilot* device), we do window slicing on the raw eye-tracking data, extract relevant features and use baseline subtraction. We split the data into 80% analysis and 20% test data. With the analysis data, we optimize classification pipelines using Naive AutoML [28] (Sec. III-A) and evaluate the pipelines on the test data (Sec. III-B). Next, we investigate the influence of the number of active robots (Sec. III-C) and the experimental duration (Sec. III-D). Finally, we explore potential for fine tuning models to the individual user (Sec. III-E).

A. Optimizing ML pipelines for eye-tracking data

To determine the optimal ML pipeline, we use the analysis dataset and maximize accuracy as the evaluation metric. We optimize one ML pipeline for each time window size t_w for 2 or 3 classes, obtaining a total of 32 optimization settings. The optimization results using the *duration estimate* label can be found in Table I and for the *PPOT* label in Table II. The

TABLE I: Optimization results for the *duration estimate* labeled analysis dataset.

t_w [s]	2 classes			3 classes		
	Pre	Clf	ACC	Pre	Clf	ACC
1	None	ETC	0.983	None	ETC	0.970
2	None	RFC	0.987	PCA	RFC	0.973
5	VT	RFC	0.979	None	RFC	0.970
10	None	RFC	0.953	VT	RFC	0.949
15	None	RFC	0.946	VT	RFC	0.908
20	None	ETC	0.906	VT	ETC	0.863
30	VT	ETC	0.877	VT	ETC	0.836
45	VT	ETC	0.843	None	ETC	0.789
60	VT	ETC	0.800	VT	ETC	0.717

TABLE II: Optimization results for the *PPOT* labeled analysis dataset.

t_w [s]	2 classes			3 classes		
	Pre	Clf	ACC	Pre	Clf	ACC
1	NOR	ETC	0.973	NOR	ETC	0.975
2	PCA	kNN	0.974	VT	RFC	0.975
5	PCA	kNN	0.953	None	RFC	0.975
10	NOR	ETC	0.923	VT	ETC	0.931
15	NOR	ETC	0.908	VT	ETC	0.893
20	None	ETC	0.894	VT	ETC	0.853
30	None	ETC	0.870	VT	ETC	0.825
45	None	ETC	0.827	VT	ETC	0.769
60	None	ETC	0.791	PCA	ETC	0.710

exact hyperparameter choices can be found in the implementation. Throughout all different settings we see that the optimizer most often chose the *RandomForestClassifier* (RFC) or *ExtraTreesClassifier* (ETC) as classifiers (CLF), while for few settings the *KNeighborsClassifier* (kNN) was chosen. The most often selected preprocessing step (PRE) is *VarianceThreshold* (VT), followed by principal component analysis (PCA), and *Normalizer* (NOR). No preprocessing step (None) was chosen 11 times over the 32 optimizing settings. Given we converge to the same models, suggests that these models effectively capture the underlying dataset structure and that the dataset is sufficiently large to mitigate the impact of noise from random data splits and stochastic model initialization. We observe that the better results are obtained using smaller time window sizes t_w , which could be due to the larger datasets. For a smaller time window size, we can extract more samples. The samples also have a higher correlation as the physiology of the human eye changes with finite speed.

B. Evaluating optimized ML pipelines on the test dataset

Next, we evaluate the optimized ML pipelines from the previous section using the unseen test dataset. We do 100 independent iterations, training with 80% of the analysis data (stratified split) and all features, and then classify all test data samples. The classification results of the test data using the *duration estimate* and *PPOT* label can be found in Table III. The results on the unseen test data show that we are able to classify the subjective time perception, either measured through *duration estimation* or *PPOT*, based on the eye-tracking data with a high accuracy for all settings.

TABLE III: Classification accuracies of unseen test data for *duration estimation* and *PPOT* labels (\pm standard deviation).

t_w [s]	2 classes		3 classes	
	<i>duration estimate</i>	<i>PPOT</i>	<i>duration estimate</i>	<i>PPOT</i>
1	0.983 \pm 0.003	0.950 \pm 0.002	0.973 \pm 0.003	0.961 \pm 0.003
2	0.985\pm0.001	0.972\pm0.002	0.979\pm0.002	0.974\pm0.002
5	0.972 \pm 0.002	0.953 \pm 0.002	0.970 \pm 0.001	0.964 \pm 0.002
10	0.954 \pm 0.005	0.919 \pm 0.004	0.951 \pm 0.004	0.947 \pm 0.003
15	0.944 \pm 0.004	0.914 \pm 0.007	0.936 \pm 0.006	0.917 \pm 0.006
20	0.917 \pm 0.006	0.880 \pm 0.007	0.867 \pm 0.011	0.845 \pm 0.007
30	0.851 \pm 0.012	0.837 \pm 0.010	0.778 \pm 0.015	0.780 \pm 0.014
45	0.864 \pm 0.018	0.833 \pm 0.015	0.759 \pm 0.016	0.736 \pm 0.013
60	0.809 \pm 0.020	0.846 \pm 0.013	0.709 \pm 0.026	0.701 \pm 0.022

The comparable performance, achieved using the full dataset and the analysis dataset, suggests that the models have effectively captured a robust representation of the underlying data structure. Similar to the results using the analysis dataset to optimize the ML pipelines (Table I and Table II), we observe that the classification performance increases for smaller time windows t_w . This can again be attributed to the larger datasets, which provide more training data that closely resemble the test data, as the temporal differences and consequently the variances are smaller. This is because the human eye physiology changes in the range of milliseconds to seconds. Further, the performance decrease for larger t_w is not explainable by variations in the class distribution, as for the two class datasets the variation is within 3% (majority class using *duration estimate*: 59% for $t_w = 2$ s, 56% for $t_w = 60$ s; majority class using *PPOT*: 69% for $t_w = 2$ s, 66% for $t_w = 60$ s). For the three class datasets, the variation is within 4% (majority class using *duration estimate*: 45% for $t_w = 2$ s, 41% for $t_w = 60$ s; majority class using *PPOT*: 43% for $t_w = 2$ s, 44% for $t_w = 60$ s). This is in contrast to [22] who found the 20 s time window to work best.

For our desired task, obtaining online feedback for a *ChronoPilot* device, shorter time windows t_w are more desirable as feedback could be obtained faster and at higher frequency. Especially, if compared to other physiological signals used for human feedback, such as electrodermal activity or ECG, which require larger time windows or EEG, fMRI and fNIRs which are difficult to use under real world conditions, for example, working in a factory [35].

C. Influence of the number of actively moving robots

During our experimental procedure, one parameter we vary is the number of actively moving robots. The remaining (passive) robots stand still inside the arena to mitigate any side effects of varying the swarm size. To mitigate that our approach classifies for the number of actively moving robots (see [16] for label distribution for varying active robots) we split the dataset by actively moving robots (e.g., using all experiments of n actively moving robots). We use a stratified shuffle split and 100 independent repetitions. For space reasons we only present the results for binary *duration estimate* labels in Fig. 4. However, the other settings have

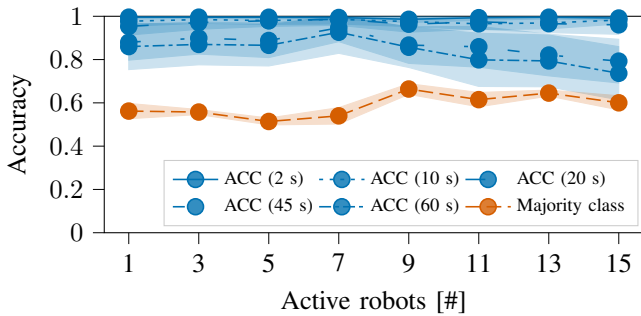


Fig. 4: Classification accuracies using the binary *duration estimate* label for experiments split by actively moving robots. The blue lines indicate the accuracy of the classifier for different t_w while the red line indicates the majority class of the subdatasets. The shaded areas represent the standard deviation (over 100 independent repetitions).

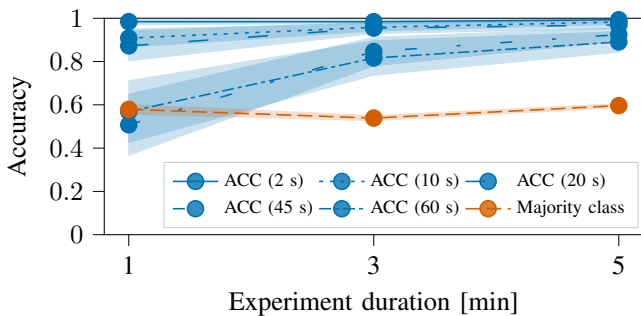


Fig. 5: Classification accuracies using the binary *duration estimate* label for experiments split by experiment duration. The blue lines indicate the accuracy of the classifier for different t_w while the red line indicates the majority class of the subdatasets. The shaded areas represent the standard deviation (over 100 independent repetitions).

qualitatively similar results. Fig. 4 shows that the classification performance is consistent regardless of the number of active robots. Hence, we assume that the ML models do not classify for the number of robots.

D. Influence of the experiment duration

The second parameter that is varied in the experiments is the experiment duration. To investigate if the experiment duration has an influence on the classification results we test our ML pipelines using only one experiment duration at a time. We use a stratified shuffle split and 100 independent repetitions. Again, for space reasons we only show the results obtained using the binary *duration estimate* labels in Fig. 5 (the other settings are qualitatively similar). Using only the 1 minute experiments we can see a dramatic decrease in performance for $t_w = \{45 \text{ s}, 60 \text{ s}\}$. This can be explained by the small dataset, as for both parameters only one sample per experiment can be generated. If we allow for ML more samples, for example, in 3 minute and 5 minute experiments, the performance goes back to normal. Similar, to the number of actively moving robots we can assume that the ML models do not classify for the experiment duration.

TABLE IV: The values are in percentage points and show by how much the fine-tuned classifier outperforms the not fine-tuned classifier.

P.ID	t_w									
	1	2	5	10	15	20	30	45	60	
2	5	20	18	20	21	25	23	23	27	
3	7	21	10	8	12	17	12	7	15	
4	20	24	19	13	11	22	16	20	28	
5	6	30	36	19	28	22	23	21	24	
6	40	47	52	39	36	29	12	22	20	
10	21	17	19	14	15	8	6	6	8	
11	10	12	9	12	7	13	8	18	18	
12	4	9	7	4	4	0	3	5	13	
13	10	12	17	13	6	6	6	9	8	
14	-1	0	2	10	13	24	18	17	7	
15	33	36	22	17	16	16	11	11	17	
16	29	33	27	20	20	15	10	11	9	
17	37	69	31	32	35	24	17	12	11	
18	3	23	12	21	25	27	12	12	14	
21	55	50	43	34	33	22	13	9	11	
22	22	32	26	11	13	6	5	7	12	
23	22	30	19	14	9	7	6	9	6	
MEAN	19	27	22	18	18	17	12	13	15	

E. Fine tuning for the individual user

For our future application of delivering human feedback to a *ChronoPilot* device, we can assume a “setup” phase that allows to collect some initial data of the current user to fine tune our models to that individual. Here, we investigate if we can fine tune the models for individual users. We use the data of the first 30 seconds of all experiments from one user combined with all data from all other users to train or adjust classifiers to this particular user. We use the remaining data of this user (e.g., 30 s from the 1 min experiment, 2:30 min of the 3 min experiment, 4:30 min of the the 5 min experiment) to evaluate the classifiers. We compare this approach to using all data of one user for testing while training on the remaining data. See Table IV for the averaged results over 100 independent repetitions of the improvement of accuracy by fine tuning the model for individual users for the binary *duration estimate* label. Depending on the user and setting, we can substantially increase the performance (up to 69%). We conclude that an initial “setup” phase can massively improve the user feedback for a *ChronoPilot* device.

IV. CONCLUSION

We have shown that we can process eye-tracking data combined with an automated ML approach to provide input to a future *ChronoPilot* device. The device would then decide autonomously over actions to modulate subject time perception. By utilizing automated ML methods we are able to find fine-tuned ML pipelines that are able to capture the properties of the underlying data. We mitigated the risk of classifiers relying on experiment-specific parameters, such as the number of actively moving robots or experiment duration. In our application scenario of providing feedback for a *ChronoPilot* device, we demonstrate that incorporating a brief “setup” phase to adjust the model to the individual user yields significant benefits.

By integrating our conceptual framework of the *ChronoPilot* device into general adaptive robotic control strategies, robot systems could dynamically adjust task complexity and interaction modalities to enhance operator performance and well-being. Future research could explore the integration of additional physiological signals with eye-tracking, incorporate multimodal feedback mechanisms, and apply our method to a broader range of collaborative human-robot scenarios. We hope to contribute to the vision of intelligent large-scale multi-robot systems that are not only efficient but also human-aware, enabling safer, more scalable, and more user-centered automation in high-demand environments.

ACKNOWLEDGMENT

This work has been partially supported by the European Union's Horizon 2020 FET research program under grant agreement 964464 (*ChronoPilot*) and the DFG under Germany's Excellence Strategy, EXC 2117, 422037984 (H.H.).

REFERENCES

- [1] J. J. McGrath *et al.*, "Age of onset and cumulative risk of mental disorders: A cross-national analysis of population surveys from 29 countries," *The Lancet Psychiatry*, vol. 10, no. 9, pp. 668–681, 2023.
- [2] R. S. Ogden, "The passage of time during the UK Covid-19 lockdown," *Plos one*, vol. 15, no. 7, p. e0235871, 2020.
- [3] J. Botev, K. Drewing, H. Hamann, Y. Khaluf, P. Simoens, and A. Vatakis, "ChronoPilot — Modulating time perception," in *2021 IEEE Int. Conf. on Artificial Intelligence and Virtual Reality (AIVR)*, 2021, pp. 215–218.
- [4] M. Cavdan, B. Celebi, and K. Drewing, "Simultaneous emotional stimuli prolong the timing of vibrotactile events," *IEEE Transactions on Haptics*, vol. 16, no. 4, pp. 622–627, 2023.
- [5] C. Schatzschneider, G. Bruder, and F. Steinicke, "Who turned the clock? Effects of manipulated Zeitgebers, cognitive load and immersion on time estimation," *IEEE Transactions on Visualization and Computer Graphics*, vol. 22, no. 4, pp. 1387–1395, 2016.
- [6] S. Picard and J. Botev, "Rhythmic stimuli effects on subjective time perception in immersive virtual environments," in *Proc. of the 14th Int. Workshop on Immersive Mixed and Virtual Environment Systems*, 2022, pp. 5–11.
- [7] J. Kaduk, M. Cavdan, K. Drewing, A. Vatakis, and H. Hamann, "Effects of human-swarm interaction on subjective time perception: Swarm size and speed," in *Proc. of the 2023 ACM/IEEE Int. Conf. on Human-Robot Interaction*, 2023, pp. 456–465.
- [8] T. Aust, E. Balta, A. Vatakis, and H. Hamann, "Automatic classification of subjective time perception using multi-modal physiological data of air traffic controllers," in *2024 IEEE Int. Conf. on Systems, Man, and Cybernetics (SMC)*, 2024, pp. 3962–3967.
- [9] L. Orlandic, A. A. Valdes, and D. Atienza, "Wearable and continuous prediction of passage of time perception for monitoring mental health," in *2021 IEEE 34th Int. Symposium on Computer-Based Medical Systems (CBMS)*, 2021, pp. 444–449.
- [10] F. Chen, J. Zhou, Y. Wang, K. Yu, S. Z. Arshad, A. Khawaji, and D. Conway, *Robust multimodal cognitive load measurement*. Springer, 2016.
- [11] H. Hamann, *Swarm robotics: A formal approach*. Springer, 2018.
- [12] M. Dorigo, G. Theraulaz, and V. Trianni, "Swarm robotics: Past, present, and future [point of view]," *Proc. of the IEEE*, vol. 109, no. 7, pp. 1152–1165, 2021.
- [13] J. Y. C. Chen, M. J. Barnes, and M. Harper-Sciarni, "Supervisory control of multiple robots: Human-performance issues and user-interface design," *IEEE Transactions on Systems, Man, and Cybernetics, Part C (Applications and Reviews)*, vol. 41, no. 4, pp. 435–454, 2010.
- [14] M. Divband Soorati, J. Clark, J. Ghofrani, D. Tarapore, and S. D. Ramchurn, "Designing a user-centered interaction interface for human-swarm teaming," *Drones*, vol. 5, no. 4, p. 131, 2021.
- [15] G. Podevijn, R. O'Grady, N. Mathews, A. Gilles, C. Fantini-Hauwel, and M. Dorigo, "Investigating the effect of increasing robot group sizes on the human psychophysiological state in the context of human-swarm interaction," *Swarm Intelligence*, vol. 10, no. 3, pp. 193–210, 2016.
- [16] J. Kaduk, M. Cavdan, K. Drewing, and H. Hamann, "From one to many: How active robot swarm sizes influence human cognitive processes," in *2024 33rd IEEE Int. Conf. on Robot and Human Interactive Communication (ROMAN)*, 2024, pp. 1207–1212.
- [17] G. Dietz, J. L. E. P. Washington, L. H. Kim, and S. Follmer, "Human perception of swarm robot motion," in *Proc. of the 2017 CHI Conf. Extended Abstracts on Human Factors in Computing Systems*, 2017, pp. 2520–2527.
- [18] Z. Qian, L. Orlov Savko, C. Neubauer, G. Gremillion, and V. Unhelkar, "Measuring variations in workload during human-robot collaboration through automated after-action reviews," in *Companion of the 2024 ACM/IEEE Int. Conf. on Human-Robot Interaction*, 2024, pp. 852–856.
- [19] V. Villani, B. Capelli, C. Secchi, C. Fantuzzi, and L. Sabattini, "Humans interacting with multi-robot systems: A natural affect-based approach," *Autonomous Robots*, vol. 44, pp. 601–616, 2020.
- [20] J. Z. Lim, J. Mountstephens, and J. Teo, "Eye-tracking feature extraction for biometric machine learning," *Frontiers in neurorobotics*, vol. 15, p. 796895, 2022.
- [21] K. Tao, Y. Huang, Y. Shen, and L. Sun, "Automated stress recognition using supervised learning classifiers by interactive virtual reality scenes," *IEEE Transactions on Neural Systems and Rehabilitation Engineering*, vol. 30, pp. 2060–2066, 2022.
- [22] Y. Guo, D. Freer, F. Deligianni, and G.-Z. Yang, "Eye-tracking for performance evaluation and workload estimation in space telerobotic training," *IEEE Transactions on Human-Machine Systems*, vol. 52, no. 1, pp. 1–11, 2022.
- [23] J. Z. Lim, J. Mountstephens, and J. Teo, "Emotion recognition using eye-tracking: Taxonomy, review and current challenges," *Sensors*, vol. 20, no. 8, p. 2384, 2020.
- [24] Q. Yao, M. Wang, Y. Chen, W. Dai, Y.-F. Li, W.-W. Tu, Q. Yang, and Y. Yu, "Taking human out of learning applications: A survey on automated machine learning," *arXiv preprint arXiv:1810.13306*, vol. 31, 2018.
- [25] M. Feurer, A. Klein, K. Eggensperger, J. Springenberg, M. Blum, and F. Hutter, "Efficient and robust automated machine learning," in *Advances in Neural Information Processing Systems* 28, 2015, pp. 2962–2970.
- [26] M. Feurer, K. Eggensperger, S. Falkner, M. Lindauer, and F. Hutter, "Auto-sklearn 2.0: Hands-free automl via meta-learning," *Journal of Machine Learning Research*, vol. 23, no. 261, pp. 1–61, 2022.
- [27] P. Gijssbers and J. Vanschoren, "GAMA: Genetic automated machine learning assistant," *Journal of Open Source Software*, vol. 4/33, 2019.
- [28] F. Mohr and M. Wever, "Naive automated machine learning," *Machine Learning*, vol. 112, pp. 1131–1170, 2022.
- [29] F. Riedo, M. Chevalier, S. Magnenat, and F. Mondada, "Thymio II, a robot that grows wiser with children," in *2013 IEEE Workshop on Advanced Robotics and its Social Impacts*, 2013, pp. 187–193.
- [30] R. L. Piferi, K. A. Kline, J. Younger, and K. A. Lawler, "An alternative approach for achieving cardiovascular baseline: Viewing an aquatic video," *Int. Journal of Psychophysiology*, vol. 37/2, pp. 207–217, 2000.
- [31] C. Kothe, S. Y. Shirazi, T. Stenner, D. Medine, C. Boulay, M. I. Grivich, T. Mullen, A. Delorme, and S. Makeig, "The lab streaming layer for synchronized multimodal recording," *BioRxiv*, 2024.
- [32] A. T. Duchowski, K. Krejtz, I. Krejtz, C. Biele, A. Niedzielska, P. Kiefer, M. Raubal, and I. Giannopoulos, "The index of pupillary activity: Measuring cognitive load vis-à-vis task difficulty with pupil oscillation," in *Proc. of the 2018 CHI Conf. on Human Factors in Computing Systems*, 2018, pp. 1–13.
- [33] H. Lejeune and J. H. Wearden, "Vierordt's the experimental study of the time sense (1868) and its legacy," *European Journal of Cognitive Psychology*, vol. 21, no. 6, pp. 941–960, 2009.
- [34] F. Pedregosa, G. Varoquaux, A. Gramfort, V. Michel, B. Thirion, O. Grisel, M. Blondel, P. Prettenhofer, R. Weiss, V. Dubourg, J. Vanderplas, A. Passos, D. Cournapeau, M. Brucher, M. Perrot, and E. Duchesnay, "Scikit-learn: Machine learning in Python," *Journal of Machine Learning Research*, vol. 12, pp. 2825–2830, 2011.
- [35] D. Das Chakladar and P. P. Roy, "Cognitive workload estimation using physiological measures: A review," *Cognitive Neurodynamics*, vol. 18, pp. 1445–1465, 2024.